Characterisation of Cu2O/CuO thin films produced by plasma-assisted DC sputtering for solar cell application

Alajlani, Yahya; Placido, Frank; Chu, Hin On; De Bold, Robert; Fleming, Lewis; Gibson, Desmond

Published in:
Thin Solid Films

DOI:
10.1016/j.tsf.2017.09.023

E-pub ahead of print: 13/09/2017

Document Version
Peer reviewed version

Characterisation of Cu2O/CuO thin films produced by plasma-assisted DC sputtering for solar cell application

Yahya Alajlani, Frank Placido, Hin On Chu, Robert De Bold, Lewis Fleming, Des Gibson

PII: S0040-6090(17)30692-2
DOI: doi: 10.1016/j.tsf.2017.09.023
Reference: TSF 36225

To appear in: *Thin Solid Films*

Received date: 28 January 2017
Revised date: 7 September 2017
Accepted date: 12 September 2017

Please cite this article as: Yahya Alajlani, Frank Placido, Hin On Chu, Robert De Bold, Lewis Fleming, Des Gibson , Characterisation of Cu2O/CuO thin films produced by plasma-assisted DC sputtering for solar cell application, *Thin Solid Films* (2017), doi: 10.1016/j.tsf.2017.09.023

Characterisation of Cu_2O/CuO thin films produced by plasma-assisted DC sputtering for solar cell application

Yahya Alajlani[1, 2], Frank Placido[1], Hin On Chu[1], Robert De Bold[3], Lewis Fleming[1], Des Gibson[1].

[1]Scottish Universities Physics Alliance (SUPA), Institute of Thin Films, Sensors and Imaging, University of the West of Scotland, UK

[2]Jazan University, Faculty of Science, Physics Department, Jazan, Suadi Arabia

[3]Institute for Infrastructure and Environment, School of Engineering, University of Edinburgh, Edinburgh, UK

Abstract

For large-scale implementation of devices magnetron sputtering is a practical method of producing metal oxides, however sputtered copper oxides tend to form as a mixture of Cu_2O, Cu_4O_3, and CuO, with Cu_2O being particularly difficult to produce reliably in pure form. In this study, nanostructured thin films of Cu_2O, Cu_4O_3, and CuO were prepared using a novel reactive sputtering system, based on plasma-assisted DC magnetron sputtering with deposition and plasma assisted reaction zones spatially separated enabling separate control of film oxidation. X-ray diffraction, optical spectroscopy, and Raman Spectroscopy were used to characterise the physical and optical properties and it is shown that plasma-assisted DC sputtering is a suitable technique for reliable production of CuO and Cu_2O films in large areas at room temperature without the necessity of further processing. The results also indicate that solar cell performance may relate positively to the presence of crystalline Cu_4O_3 (200) and/or Cu_2O (111) over other crystalline forms of copper oxide or amorphous copper oxide thin films.

1. Introduction

It has been noted that the development of new solar cell technology with improved efficiency and reduced costs requires production processes that use inexpensive materials and lower energy production methods [1]. The development of p-type semiconductors is one of the key technologies for future transparent electronics in applications such as displays and solar cells. Copper oxide forms three oxides, Cu_2O, Cu_4O_3, CuO. Cu_2O is widely recognised as the most promising p-type oxide because of its desirable optical and electrical properties. Therefore, copper oxide is an attractive material choice for solar cell applications because it is inexpensive, non-toxic, abundant, has an absorption coefficient within the visible spectrum, and is a natural p-type semiconductor with a direct band gap [2, 3].

Solar cells produced from copper oxide thin film have a theoretical efficiency of approximately 20 % [4, 5]; however, the best achieved efficiency to date is 8 % [6].

Copper oxide has varying optical behaviours and a range of direct optical band gaps due to stoichiometric deviations arising from the parameters and method of production [7]. That is, the deposition process to produce copper oxide thin films invariably produces a thin film containing Cu, CuO, and Cu_2O phases [8, 9].

Cu_2O thin films are noted to be slightly yellowish in appearance, highly transparent, and absorb at wavelengths less than 600 nm; whereas, CuO thin films are black in appearance, and absorb light strongly in the visible spectrum [8].

Cu_2O is particularly noted for its good electrical and optical properties in such applications in preference to CuO [10]. The direct optical band gap energy values for Cu_2O range from 2.10 eV to 2.6 eV, whereas the values for CuO range from 1.3 eV to 2.1 eV [11].

Consequently, one of the main factors in terms of improving efficiency is controlling the deposition process in order to produce a thin film from Cu_2O without a contaminating CuO phase [11]. Therefore, there is scope to improve the deposition process and consequently the efficiency of copper oxide thin film solar cells.

2. Thin Film Production Methods

There are numerous methods to produced copper oxide thin films, such as, thermal oxidation [12], electrodeposition [11], chemical brightening [7], spraying [10], chemical vapour deposition [13], plasma evaporation [10], vacuum evaporation [14], molecular beam epitaxy [15], and reactive sputtering [16]. All noted methods produce a mixture of phases of Cu, CuO, and Cu_2O [17, 18, 19, 20].

Several studies have investigated methods for depositing Cu_2O layers outlined as follows.

Balamurugan and Mehta [10] used the activated reactive evaporation technique and varied the nanocrystaline structure by varying the deposition parameters. The crystalinity was then analysed by x-ray diffractometer (XRD). The results showed that a single phase of Cu_2O could be deposited at relatively low substrate temperatures using this technique.

Papadimitropoulos et al. [14] grew copper oxide layer by vacuum evaporation of copper layers on silicon substrates in at nitrogen-oxygen atmosphere at temperatures between 185 C and 450 C. The Tauc-Lorentz model was successfully used to extract the refractive indices of the films.

Shishiyanu et al. [21] produced cuprous oxide thin films fabricated by chemical deposition and rapid photothermal processing for novel NO_2 gas sensors.

Lupan et al. [22] produced nano-crystalline copper oxide thin films via simple synthesis from chemical solutions followed by two types of thermal annealing, namely rapid thermal

annealing and conventional thermal annealing, which synthesized copper oxide nanocrystals with one and two distinctly different phases, namely Cu_2O, CuO, as well as mixed phases CuO/Cu2O. Further work by Lupan et al. [23] produced nanoplanar CuO:Zn/Cu_2O:Zn heterojunctions in nano-crystals by rapid thermal annealing. Masudy-Panah et al. [24, 25] also utilised rapid thermal annealing to improve the photocurrent performance of sputtered CuO films. Other recent CuO thin film research has investigated doping with titanium [26], aluminium [27], and nitrogen [28], with varying degrees of improvement. The nitrogen doping was found to enlarge the optical bandgap and reduce resistivity. Recent work by Perng et al. [29] produced semi-transparent Cu_2O/ZnO nanorod solar cells by electrodeposition that achieved a high short-circuit current density (J_{sc}) of 9.53 mA/cm^2.

Ogwu et al. [7] sputtered copper oxide films on glass substrates using reactive radio frequency (RF) magnetron sputtering with a copper target in an argon-oxygen atmosphere. Maximum transmission was found to be between 40 % and 80 % for copper oxide films produced with RF power of 200 W at various oxygen flow rates. The optical band gaps ranged between 2.05 eV and 2.4 eV.

Therefore, it can be seen that previous research has investigated the films produced using XRD and simulation models to determine the optical properties, and that oxygen flow rates has an influence on the transmissivity of the films produced, ie, the proportional presence of CuO and Cu_2O phases.

One method that has received little investigation in this field is plasma-assisted DC sputtering. Therefore, it is the intention of this research to determine the optimal oxygen flow rate in the plasma-assisted DC sputtering process.

3. Experimental Procedure

In this study, a plasma-assisted DC magnetron sputtering system (PlasmaCoat) [30] equipped with a 152 mm diameter circular magnetron and copper target (>99.99 %) was used for thin film deposition. A DC power supply (Advanced Energy MDX Series 1.5 kW) was used to power the target with 900 W. Another DC power supply (Advanced Energy MDX Series 500 W) was used to provide 150 W to a hollow cathode plasma source with both argon working gas and oxygen reactive gas. The PlasmaCoat has two chambers: the main chamber, where the sputtering process takes place and a load lock chamber. The substrate carousel and loadlock chamber can be seen in Figure 1a and Figure 1b respectively. The substrates are mounted on the circular holder on the side of the carousel – up to six holders can be attached to the carousel in total. Once mounted within the loadlock chamber, the carousel is able to rotate as desired for the experiment. Figure 1c shows a top view of the deposition chamber with the two magnetrons and plasma source. Figure 1d shows a diagram of the PlasmaCoat system.

The main chamber remains permanently under vacuum. The substrates are loaded onto a rotatable carousel in the load lock chamber. The main chamber and load lock chamber are separated by a gate valve. Once the load lock chamber pumps down, the rotatable carousel is automatically raised into the main process chamber and rotates at 100 RPM during deposition to ensure coating uniformity. Through the use of a roughing rotary pump and turbomolecular pump, the coating chamber rests at a base pressure of around 9×10^{-6} mBar with process pressures reaching around 5×10^{-3} mBar.

Sputtering takes place at room temperature. Sputtered copper is deposited onto the substrate which subsequently sweeps past the oxygen plasma source at the rear of the chamber, reacting to form copper oxide.

When the substrate sweeps through the oxygen plasma, as produced by the plasma-source situated at the rear of the chamber, reactive oxygen species (ROS) present in the plasma such as O_2, O_2^{1-}, O_2^{2-}, etc, chemically react with the growing metallic Cu layer, forming covalent bonds with the copper atoms resulting in the growth of a Cu_xO_y layer. By varying the rate of oxygen flow into the chamber, and therefore the oxygen plasma density, the degree of oxidation of the Cu_xO_y layer also varies, resulting in the growth of layers with different crystalline structures and stoichiometric compositions, such as those deposited and analysed in this work.

A benefit of separating sputter deposition from reaction stage is separate control of film oxidation.

Three different types of substrate were loaded: standard microscope slide substrates (30 mm by 12 mm by 1 mm thick glass) previously cleaned using an ultrasonic system (Optimal UCS40), circular silica substrates (20 mm diameter) also cleaned using an ultrasonic system (Optimal UCS40), and rectangular substrates (15 mm by 12 mm by 1 mm thick glass) coated using a MicroDyn 4000 with a 270 nm layer of indium tin oxide (ITO) under a 400 nm layer of zinc oxide (ZnO). The ITO layer was deposited under an O_2 flow of 12.5 sccm, argon flow of 190 sccm, chamber pressure of 4.1×10^{-3} Torr, DC power of 2.1 kW, 400V, 5.2 A, and microwave power of 3 W. The ZnO layer was DC sputtered for 120 minutes at 420 W, with an O_2 flow of 13 sccm, argon flow of 3sccm, a chamber pressure of 6.3×10^{-2} mBar.

The Cu_xO_y sputtering argon flow rate was 18 sccm. However, six production runs were undertaken with different oxygen flow rates: 8, 9, 10, 11, 13, 15 and 17 sccm.

Sputtering was stopped once a film thickness of 600 nm had been achieved, controlled using power/time. This approximate thickness of copper oxide has been found to be optimal in terms of photocurrent performance [24]. Afterward, a 100 nm top contact layer of gold (Au)

was applied to the rectangular substrates using a sputtering system (Quorum EMITECH-K575X Turbo Sputter Coater). Figure 2 shows the configuration of the heterojunction solar cell device.

4. Characterisation

In order to determine the crystalline structure of the copper oxide thin films, the 30 mm by 12mm glass substrates were analysed by X-ray diffractometry (XRD) and Raman spectroscopy. The XRD analysis used a Siemens D5000 with CuK α radiation (40 kV, 30 mA). The diffraction angle was set between 20 º and 60 º with 1 scan (count) per second at 0.2 increments.

Raman spectroscopy measurements were taken using a Thermo Scientific DXR Raman Microscope. Samples were measured using a 100x objective using 532 nm 1.0 mW laser excitation. Fluorescence corrections and medium cosmic ray thresholds were applied to the data collection.

In order to determine the performance of a candidate solar cell device constructed using this technique, the current-voltage (I-V) curves of the 15 mm × 12 mm glass substrates were measured using a Potentiostat/Galvanostat, Metrohm Autolab BV. Illumination was simulated AM 1.5 sunlight at 100 $mWcm^{-2}$ irradiance, generated by a Class AAA small collimated Beam Solar simulator (SF300A, Sciencetech Inc.) with the intensity calibrated by Si reference cell. The mismatch factor between the simulated sunlight and the actual solar spectrum was not corrected. The solar cells were masked with an aperture to define the active area 1 cm^2.

In order to determine the optical properties of the copper oxide thin film, the transmission and reflection spectra of the 20 mm diameter circular silica substrates were measured using an

Aquila Instruments nkd-8000 spectrometer with Pro-Optix software. Samples were all examined in S-polarized light at 10 º angle of incidence, both in transmission and reflection over the 350-1100 nm wavelength range.

Optical bandgap measurements were calculated from the transmission spectrum using the Beer-Lambert Law [31] (Eq 1) in order to determine the absorption coefficient and then Tauc's Equation [32] (Eq 2) to determine the direct optical band gap of the copper oxide thin films.

$$\alpha = \frac{1}{d}\ln\left(\frac{I_0}{I}\right) \qquad \textbf{Eq 1}$$

d = film thickness

I_0 = intensity of initial beam

I = intensity of transmitted beam

$$\alpha h\nu = A\left(h\nu - E_g\right)^{1/2} \qquad \textbf{Eq 2}$$

α = absorption coefficient

h = Plank's constant

ν = photon frequency

E_g = optical band gap

6. Results and Discussion

6.1. XRD Analysis

The XRD results of the samples can be seen in Figure 3.

The location of the spikes in intensity on the XRD plot at the various 2θ angles of incidence can be related to the material composition and crystalline orientation. The 2θ angle values for each copper composition were taken from JADE5 PDF tables and can be seen in Table 1. Consequently, it can be seen that under the various oxygen flows, the composition and orientation of the crystalline structure of the thin layers varies.

For oxygen flow rates of 15 and 13 sccm, the resultant thin films are amorphous.

For an oxygen flow rate of 17 sccm, the peaks near 35.42 º and 38.71 º indicates the presence of CuO (002) and CuO (111) respectively.

For an oxygen flow rates of 10 and 11 sccm, the peaks near 42.4 º indicates the presence of Cu_2O (200). However, the offset from 42.4 º is possibly due to slight crystalline misorientation.

For an oxygen flow rate of 9 sccm, the peak at 42.4 º indicates the presence of Cu_2O (200).

For an oxygen flow rate of 8 sccm, the small peak near 30.6 º indicates the presence of Cu_4O_3 (200), and the peak near 36.5 º indicates the presence of Cu_2O (111). Therefore the thin film produced under 8 sccm is a mixture of two copper oxides.

6.2. Raman Spectroscopy

The initial Raman measurements can be seen in Figure 4.

The initial Raman measurements showed that various phases of copper oxide were present in the thin films under different oxygen flow rates. The peaks present in the Raman measurement are indicative of each phase [33]. The presence of the various forms of copper oxide are summarised in Table 2.

It can therefore be seen from Figure 3 and Table 1 that as the oxygen flow rate increases, the oxide of copper present has a greater oxygen proportion.

6.3. Optical Analysis

Figure 5 shows the optical properties (transmittance and reflectance) of the samples across the visible spectrum (350 nm to 1100 nm).

It can be seen that from the plot that the thin film with the highest transmittance values was deposited under an oxygen flow of 9 sccm. The film produced under an oxygen flow rate of

8sccm has the lowest transmittance values of all. For flow rates between 9 and 17 sccm, the transmittance values relate inversely to oxygen flow rates: the higher the flow rate, then generally lower the transmittance value.

Reflectance values are not strongly influenced by absorption in thin films, but are used to calculate absorptance through the relationship A=1-T-R, assuming scattering in these films to be negligible.

From the calculated absorptance, it can be seen that there is high absorptance at wavelengths less than 500 nm, and the higher the oxygen flow rate, the higher the absorptance value. Above 500 nm, the absorption values are lower and optical interference fringes are observed yet with a trend for lower values. The film produced with a flow rate of 9 sccm averages a significantly lower absorption value than the rest (the thin film produced under an oxygen flow rate of 8 sccm is again an exception with a generally higher absorbtance value than the thin film produced under 11 sccm).

6.5. Solar Cell Device

In order to determine the performance of potential solar cell devices constructed using this technique, the current-voltage curve results of the films deposited on 15 mm by 12 mm glass substrates were measured and can be seen in Table 2 and Figure 5. The solar cells were measured using a Potentiostat/Galvanostat, Metrohm Autolab BV based at the University of Edinburgh Chemistry Department by colleagues who also used the same set-up and settings for their research [34]. Illumination was simulated at AM 1.5 generated by a Class AAA small collimated Beam Solar simulator (SF300A, Sciencetech Inc.) with the intensity calibrated by Si reference cell. It should be noted that the films deposited under oxygen flow rates of 15 and 17 sccm did not produce a working solar cell and, therefore, do not feature in these results.

It can be seen from Table 2 that thin films produced with an oxygen flow rate of 11 sccm or less have an energy band gap within the range for Cu_2O or Cu_4O_3 (2.1-2.6 eV). However, for greater oxygen flow rates the energy band gap decreases. It is suspected that the additional availability of oxygen leads to the formation of CuO (1.3-2.1 eV) which reduces the overal energy band gap for the thin film.

From the J-V curves in Figure 6, it can be seen that the solar cell performance of the thin films produced under oxygen flow rates of 8 sccm followed by 9 sccm have the best performances.

Given that high absorptance is necessary to produce efficient solar cells, it is therefore not intuitively obvious why cells produced with the lower oxygen flows produced the better cells. However, it can be noted that for the 8 sccm sample there was Cu_4O_3 detected by XRD and Raman, and Cu_2O detected by XRD; whereas for samples 9 sccm, 10 sccm, 11 sccm, 13 sccm, and 15 sccm, Cu_4O_3 was only detected by Raman and Cu_2O was detected by XRD and Raman (except for sample 13 sccm where Cu_2O was only detected by XRD). The PCE appears to correlate with the presence of Cu_4O_3 and Cu_2O with the 8 sccm sample having highest performance and presence of Cu_4O_3. As the oxygen flow rate increases, the presence of Cu_4O_3 declines as does the PCE, except an anomalous Raman peak in Cu_4O_3 for the 13 sccm sample that is also matched by an anomalous resurgence in PCE.

It is clear that the more oxygen rich phases of copper oxide are formed under higher oxygen flows.

It is notable that the thin film that did not function as a solar cell (15 sccm) was suspected of having CuO present due to the higher availability of oxygen in the production process compared to the other thin films. The presence of CuO would prevent the solar cell from functioning.

These results indicate that solar cell performance may relate positively to the presence of crystalline Cu_4O_3 (200) and/or Cu_2O (111) over other crystalline forms of copper oxide or amorphous copper oxide thin films.

7. Conclusions

In general, in terms of visible light (350 nm-700 nm), it appears that the thin films produced with higher oxygen flows have higher absorptance and lower reflectance values. The Raman results indicate samples deposited under higher oxygen flow rates have a greater presence of more oxygen rich phases of copper oxide – the most oxygen rich, CuO, is black and highly absorbent of visible light and is present in the most absorptant thin films that were produced under the highest oxygen flow rates (15 and 17 sccm).

In terms of performance as a solar cell, it is apparent that greater performance is derived from those composed of a copper oxide thin films deposited under a flow rate of 8 sccm or 9 sccm. The XRD result previously confirmed the presence of Cu_2O in the thin film produced under an oxygen flow rate of 8 sccm, and the XRD and Raman results previously confirmed the presence of Cu_2O in the thin film produced under an oxygen flow rate of 9 sccm. With increasing oxygen flow rates in the production of the thin film, the solar cell performance appears to decrease. Although the cell performances in terms of percentage conversion efficienies (PCE) are very low, the solar cells serve as proof-of-concept devices for the method.

Acknowledgements

The author would like to thank Professor Neil Robertson of the University of Edinburgh School of Chemistry for providing access to solar cell testing equipment, and Dr Aruna Ivaturi of the University of Edinburgh School of Chemistry for laboratory assistance.

Figure 1a Substrate carousel [30]

Figure 1b Substrate carousel mounted within loadlock chamber [30]

Figure 1c Top view of deposition chamber with two magnetrons (6 ” diameter) and plasma source [30]

Figure 1d Diagram of PlasmaCoat system

Figure 2 Heterojunction solar cell device configuration

Figure 3 XRD of samples deposited under various oxygen flows

Table 1 2θ angles for XRD of plasma-assisted DC sputtered copper oxide films

Figure 4 Raman microscope measurements of thin film produced by plasma-assisted DC at various oxygen flow rates

Table 2 Interpretation of copper oxide content based on Raman observations

a

b

c

Figure 5 Optical properties of samples deposited under various oxygen flows (a – transmittance with Eg values, b - reflectance, and c - absorptance)

Table 3 J-V curve and E-gap measurements

a

b

Figure 6 Current-voltage measurement of samples deposited under various oxygen flows (a – dark case, b – light case)

References

[1] S. S. Jeong, A. Mittiga, E. Salza, A. Masci and S. Passerini, “Electrodeposited ZnO/Cu2O heterojunction solar cells,” Electrochimica Acta, vol. 53, pp. 2226-2231, 2008.

[2] F. Oba, F. Ernst, Y. Yu, R. Liu, H. M. Kothari and J. A. Switxer, “Epitaxial growth of cuprous oxide electrodeposited onto semiconductor and metal substrates,” Journal of the American Ceramic Society, vol. 88, no. 2, pp. 253-270, 2005.

[3] K. Akimoto, S. Ishizuka, M. Yanagita, Y. Nawa, G. K. Paul and T. Sakurai, “Thin film deposition of Cu2O and application for solar cells,” Solar Energy, vol. 80, no. 6, pp. 715-722, 2006.

[4] J. J. Loferski, “Theoretical considerations governing the choice of the optimum semiconductor for photovoltaic solar energy conversion,” Jouurnal of Applied Physics, vol. 27, no. 7, pp. 777-784, 1956.

[5] L. C. Olsen, R. C. Bohara and M. W. Urie, “Explanation for low-efficiency Cu2O Schottky-barrier solar cells,” Applied Physics Letters, vol. 34, no. 1, p. 47, 1979.

[6] T. Minami, Y. Nishi and T. and Miyata, “Efficiency enhancement using a Zn1− x Ge x-O thin film as an n-type window layer in Cu2O-based heterojunction solar cells,” Applied Physics Express, vol. 9, no. 5, p. 052301, 2016.

[7] A. A. Ogwu, E. Bouquerel, O. Ademosu, S. Moh, E. Crossan and F. Placido, “An investigation of the surface energy and optical transmittance of copper oxide thin films by reactive magnetron sputtering,” Acta Materialia, vol. 53, pp. 5151-5159, 2005b.

[8] T. J. Richardson, J. L. Slack and M. D. Rubin, “Electrochromism of copper oxide thin films,” Electrochimica Acta, vol. 46, pp. 2281-2284, 2001.

[9] H. Derin and K. Kantarli, “Optical characterization of thin thermal oxide films on copper by ellipsometry,” Applied Physics A , vol. 75, no. 3, pp. 391-395, 2002.

[10] B. Balamurugan and B. R. Mehta, “Optical and structural properties of nanocrystalline copper oxide thin films prepared by activated reactive evaporation,” Thin solid films, vol. 96, no. 1, pp. 90-96, 2001.

[11] A. A. Ogwu, E. Bouquerel, O. Ademosu, S. Moh, E. Crossan and F. Placido, “The influence of RF power and oxygen flow rate during deposition on the optical transmittance of copper oxide thin films prepared by reactive magnetron sputtering,” Journal of Physics D: Applied Physics, vol. 38, pp. 266-271, 2005a.

[12] K. Ozawa, Y. Oba and K. Edamoto, “Formation and characterization of the Cu2O overlayer on Zn(0001),” Surface Science, vol. 603, no. 13, pp. 2163-2170, 2009.

[13] S. C. Ray, “Preparation of copper oxide thin film by the sol–gel-like dip technique and study of their structural and optical properties,” Solar energy materials and solar cells, vol. 68, pp. 307-312, 2001.

[14] G. N. Papadimitropoulos, N. Vourdas, E. Vamvakas and D. Davazoglou, “Optical and structural properties of copper oxide thin films grown byoxidation of metal layers,” Thin Solid Films, vol. 515, p. 2428–2432, 2006.

[15] R. Kita, T. Hase, R. Itti, M. Sasaki, T. Morishita and S. Tanaka, “Synthesis of cupric oxide films using mass-separated low-energy beam,” Applied Physica Letters, vol. 60, pp. 2624-2630, 1992.

[16] V. F. Drobny and D. L. Pulfrey, “Properties of reactively-sputtered Copper Oxide thin films,” Thin Solid Films, vol. 61, pp. 89-98, 1979.

[17] K. Santra, C. K. Sarkar, M. K. Mukherjee and B. Ghosh, “Copper oxide thin films grown by plasma evaporation method,” Thin Solid Films, vol. 213, no. 2, pp. 226-229, 1992.

[18] R. Padiyath, J. Seth and S. V. Babu, “Deposition of copper oxide films by reactive laser ablation of copper formate in an rf oxygen plasma ambient,” Thin Solid Films, vol. 239, no. 1, pp. 8-15, 1994.

[19] K. H. Yoon, W. J. Choi and D. H. Kang, “Photoelectrochemical properties of copper oxide thin films coated on an n-Si substrate,” Thin Solid Films, vol. 372, no. 1, pp. 250-256., 2000.

[20] P. Luzeau, X. Z. Xu, M. Lagues, N. C. J. P. Hess, M. Nanot, F. Queyroux, M. Touzeau and D. Pagnon, “Copper oxide thin-film growth using an oxygen plasma source,” Journal of Vacuum Science & Technology A: Vacuum, Surfaces, and Films, vol. 8, no. 6, pp. 3938-3940, 1990.

[21] S. T. Shishiyanu, T. S. Shishiyanu and O. I. Lupan, “Novel NO2 gas sensor based on cuprous oxide thin films,” Sensors and Actuators B: Chemical, vol. 113, no. 1, pp. 468-476, 2006.

[22] O. Lupan, V. Cretu, V. Postica, N. Ababii, O. Polonskyi, V. Kaidas, F. Schütt, Y. K. Mishra, E. Monaico, I. Tiginyanu and V. Sontea, “Enhanced ethanol vapour sensing performances of copper oxide nanocrystals with mixed phases,” Sensors and Actuators B: Chemical, vol. 224, pp. 434-448, 2016a.

[23] Lupan, V. Cretu, V. Postica, O. Polonskyi, N. Ababii, F. Schütt, V. Kaidas, F. Faupel and R. Adelung, “Non-planar nanoscale p–p heterojunctions formation in ZnxCu 1− x Oy nanocrystals by mixed phases for enhanced sensors,” Sensors and Actuators B: Chemical, vol. 230, pp. 832-843, 2016b.

[24] S. Masudy-Panah, R. S. Moakhar, C. S. Chua, A. Kushwaha, T. I. Wong and G. K. Dalapati, “Rapid thermal annealing assisted stability and efficiency enhancement in a sputter deposited CuO photocathode,” RSC Advances, vol. 6, no. 35, pp. 29383-29390, 2016.

[25] S. Masudy-Panah, G. K. Dalapati, K. Radhakrishnan, A. Kumar, H. R. Tan, E. Naveen Kumar, C. Vijila, C. C. Tan and D. Chi, "p-CuO/n-Si heterojunction solar cells with high open circuit voltage and photocurrent through interfacial engineering," Progress in Photovoltaics: Research and Applications, vol. 23, no. 5, pp. 637-645, 2015.

[26] S. Masudy-Panah, K. Radhakrishnan, H. R. Tan, R. Yi, T. I. Wong and G. K. Dalapati, "Titanium doped cupric oxide for photovoltaic application," Solar Energy Materials and Solar Cells, vol. 140, pp. 266-274, 2015.

[27] S. Masudy-Panah, K. Radhakrishnan, T. H. Ru, R. Yi, T. I. Wong and G. K. Dalapati, "In situ codoping of a CuO absorber layer with aluminum and titanium: the impact of codoping and interface engineering on the performance of a CuO-based heterojunction solar cell," Journal of Physics D: Applied Physics, vol. 49, no. 37, p. 375601, 2016.

[28] S. Masudy-Panah, K. Radhakrishnan, A. Kumar, T. I. Wong, R. Yi and G. K. Dalapati, "Optical bandgap widening and phase transformation of nitrogen doped cupric oxide," Journal of Applied Physics, vol. 118, no. 22, p. 225301, 2015.

[29] D. C. Perng, M. H. Hong, K. H. Chen and K. H. Chen, "Enhancement of short-circuit current density in Cu 2 O/ZnO heterojunction solar cells," Journal of Alloys and Compounds, vol. 695, pp. 549-554, 2017.

[30] D. Gibson, J. Martin, F. Placido and D. Child, "Magnetron sputtering system for small batch high throughput production," 55th Annual Technical Conference Proceedings, Santa Clara, CA 28 April - 3 May, Society of Vacuum Coaters vol. 505, paper 856-7188, 2012.

[31] J. H. Lambert, Photometria sive de mensura et gradibus luminis, colorum et umbrae, Klett, 1760.

[32] J. Tauc, "Optical properties and electronic structure of amorphous Ge and Si," Materials Research Bulletin, vol. 3, pp. 37-46, 1968.

[33] L. Debbichi, M. C. Marco, D. Lucas, F. J. Pierson and P. Krüger, "Vibrational properties of CuO and Cu4O3 from first-principles calculations, and Raman and Infrared Spectroscopy," The Journal of Physical Chemistry C, vol. 116, pp. 10232-10237, 2012.

[34] M. Maciejczyk, A. Ivaturia and N. Robertson, "SFX as a low-cost 'Spiro' hole-transport material for efficient perovskite solar cells," Journal of Materials Chemistry A, vol. 4, pp. 4855-4863, 2016.

Table 1

Phase	Angle	Reference
Cu_4O_3 (200)	30.6 °	JADE5 PDF Table: PDF#49-1830
CuO (002)	35.4 °	JADE5 PDF Table: PDF#48-1548
Cu_4O_3 (202)	35.8 °	JADE5 PDF Table: PDF#49-1830
Cu_4O_3 (004)	36.3 °	JADE5 PDF Table: PDF#49-1830
Cu_2O (111)	36.5 °	JADE5 PDF Table: PDF#65-3288
CuO (111)	38.7 °	JADE5 PDF Table: PDF#48-1548
Cu_2O (200)	42.4 °	JADE5 PDF Table: PDF#65-3288
Cu_4O_3 (220)	44.0 °	JADE5 PDF Table: PDF#49-1830

Table 2

O_2 Flow Rate (sccm)	Cu_2O	Cu_4O_3	CuO
8	None	Present	None
9	Present	Present	None
10	Present	Present	None
11	Present	Present	None
13	None	Present	None
15	None	Present	Present
17	None	None	Present

Table 3

Oxygen Flow (sccm)	**Energy Band Gap Eg (eV)**	**Voc (Volts)**	**J_{sh} (mA/cm^2)**	**Fill Factor**	**PCE (%)**
8	2.00	0.19	0.008	0.26	0.040
9	2.37	0.11	0.004	0.15	0.012
10	2.32	0.08	0.0005	0.11	0.000
11	2.21	0.09	0.002	0.26	0.002
13	1.95	0.04	0.002	0.23	0.009
15	1.84	-	-	-	-
17	1.81	-	-	-	-

Figure 1a

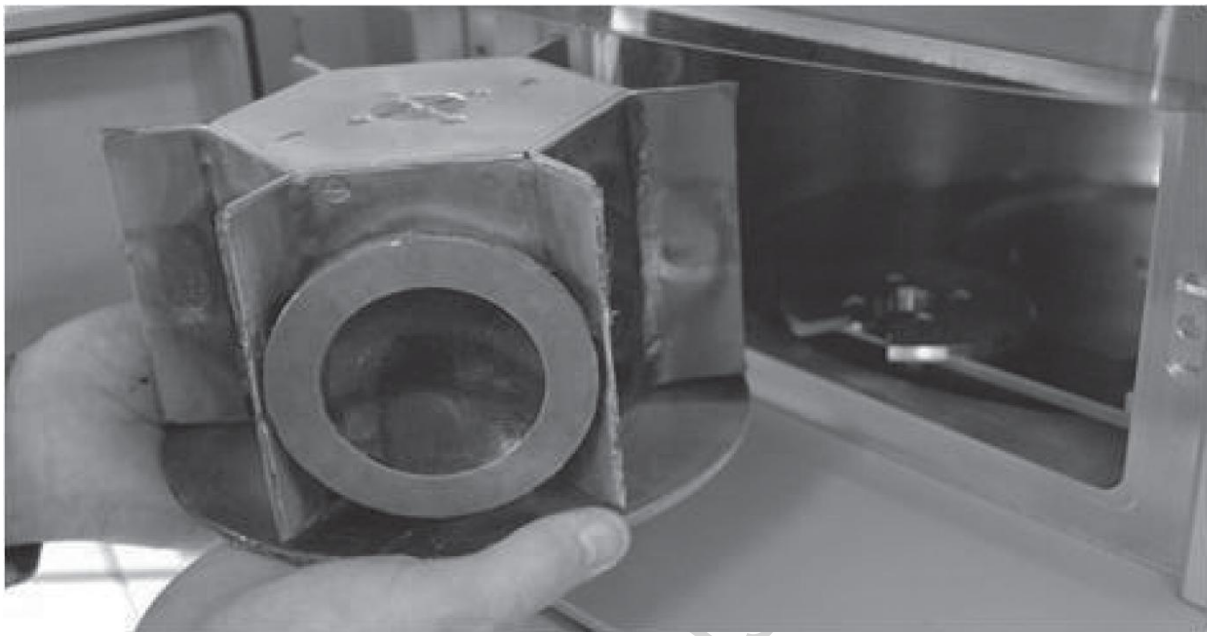

Figure 1b

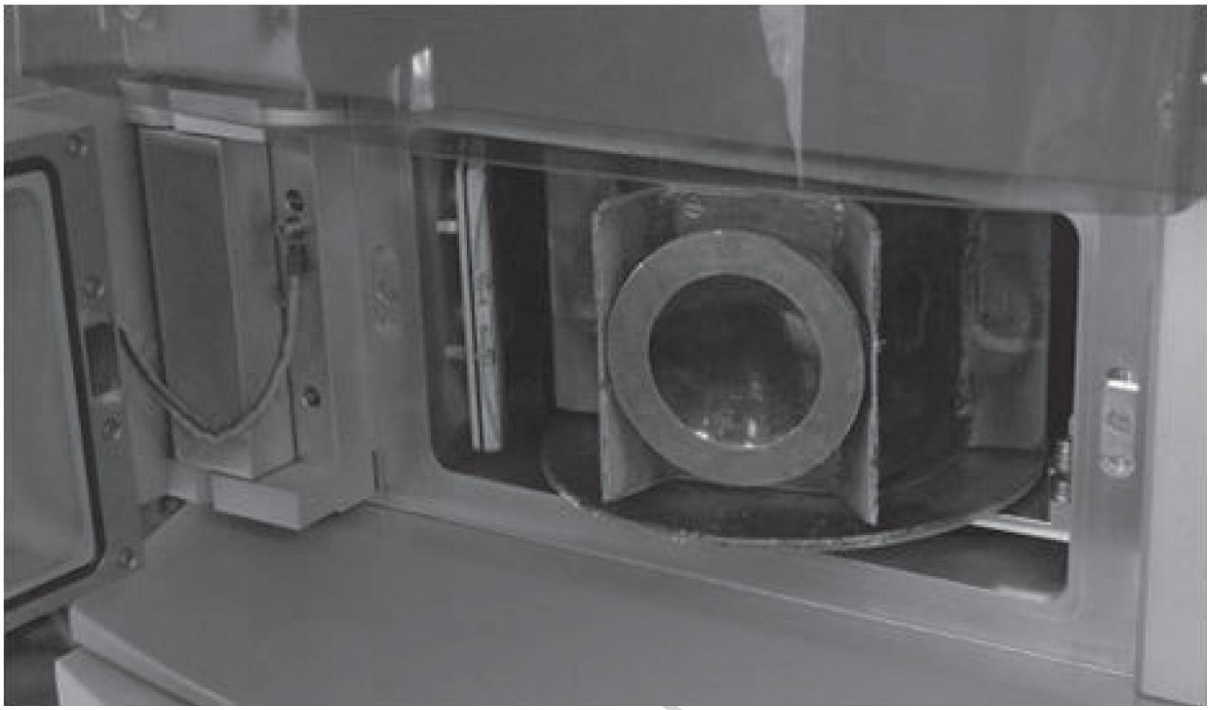

Figure 1c

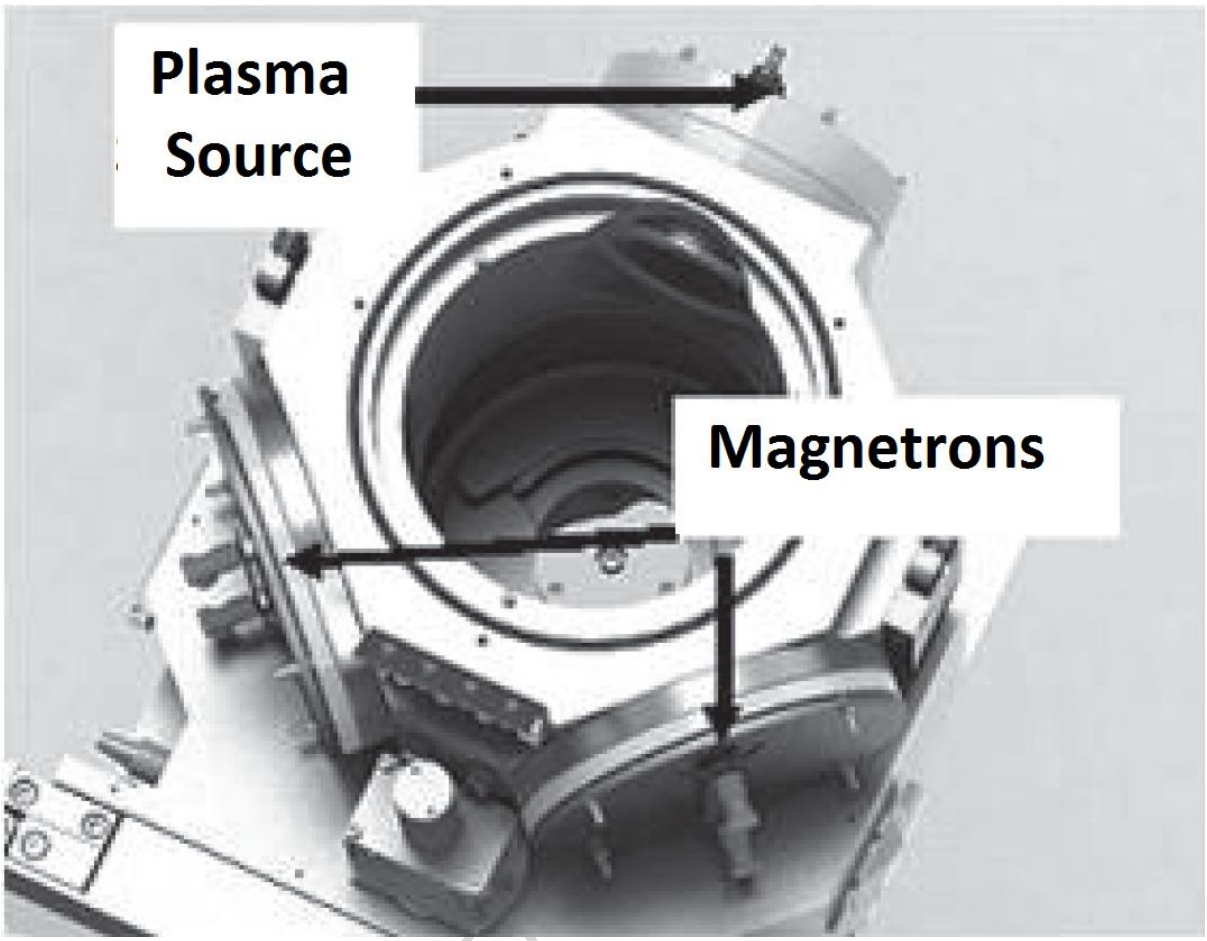

Figure 1d

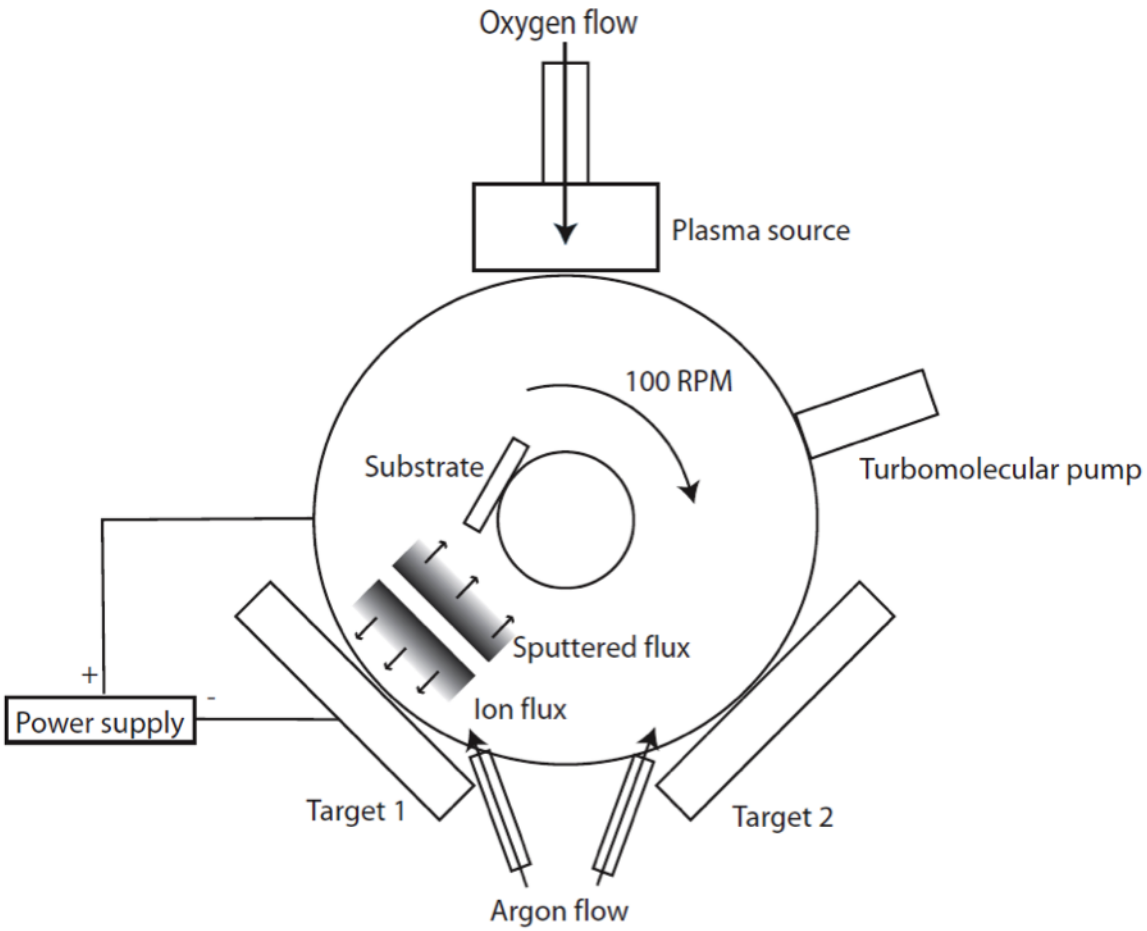

Figure 2

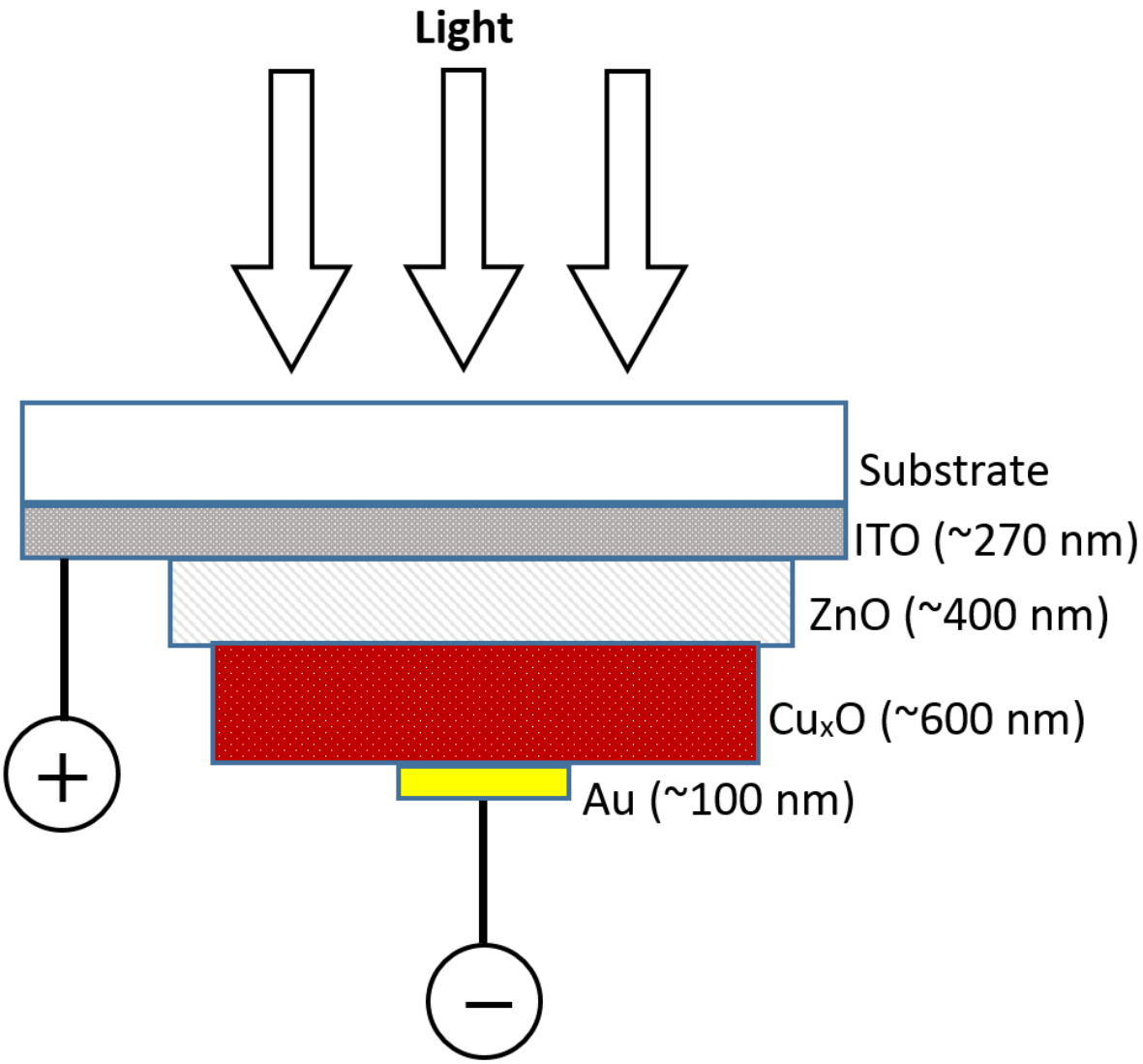

Figure 3

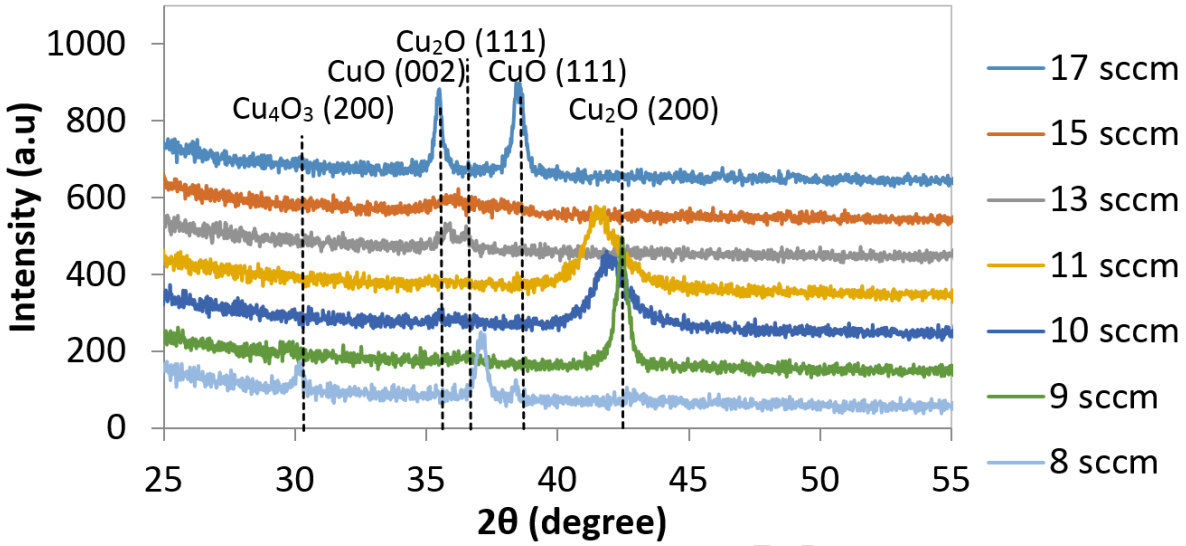

Figure 4

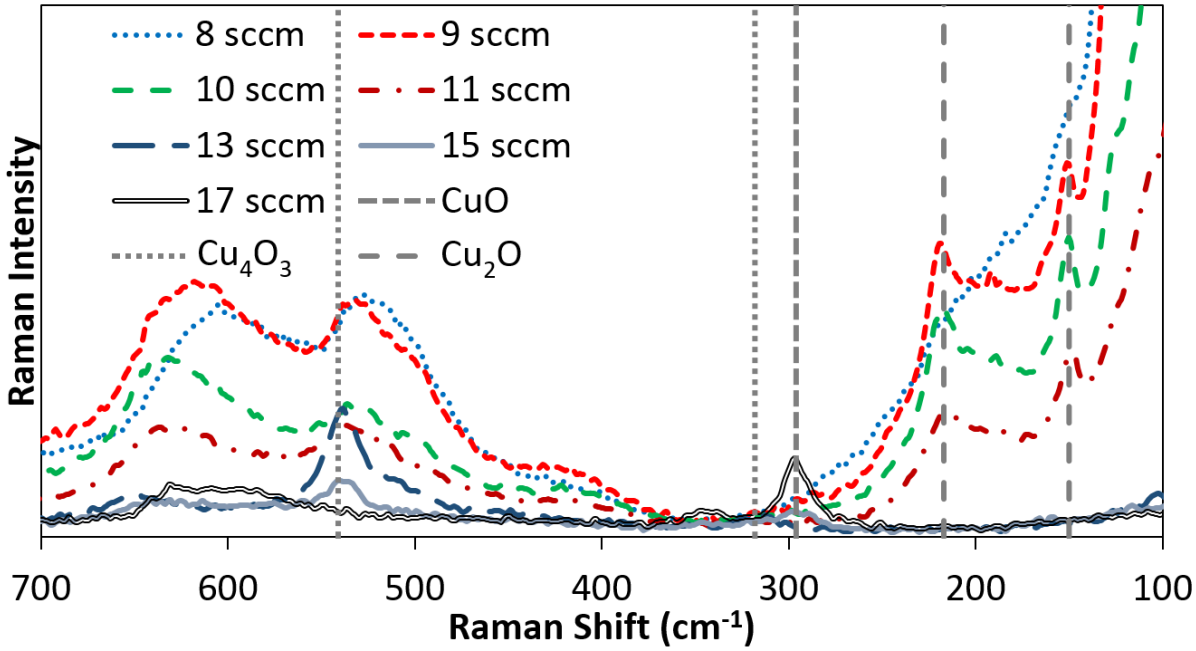

Figure 5a

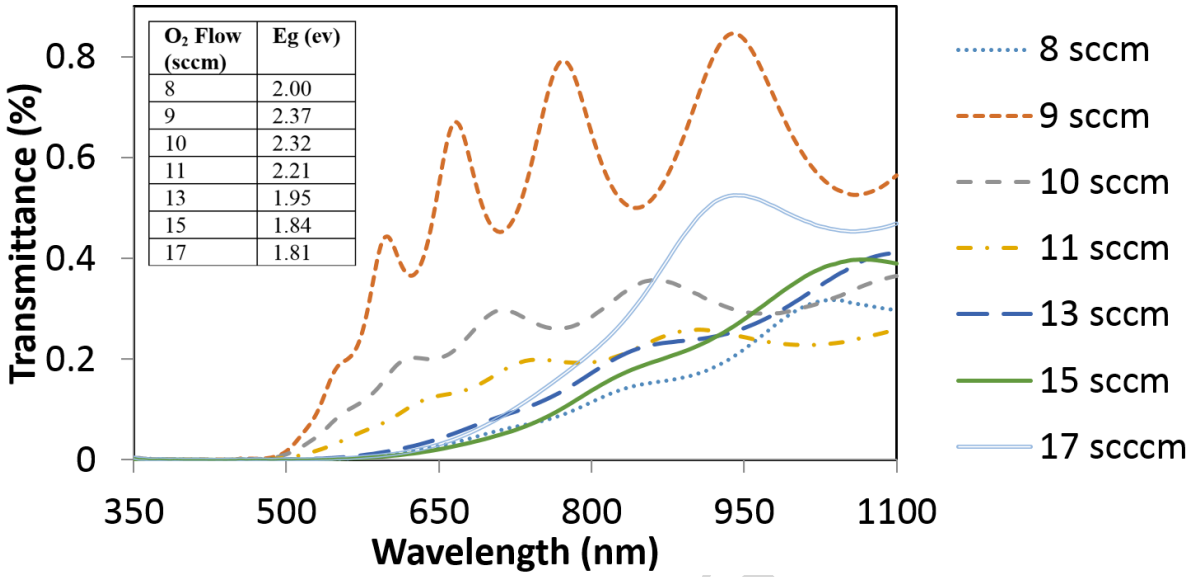

Figure 5b

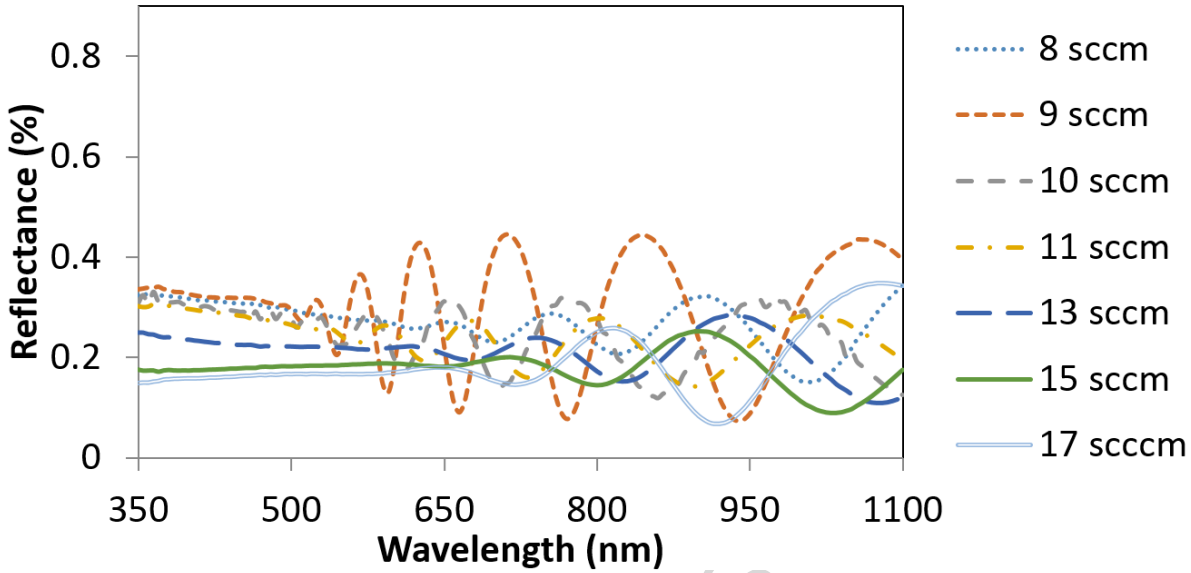

Figure 5c

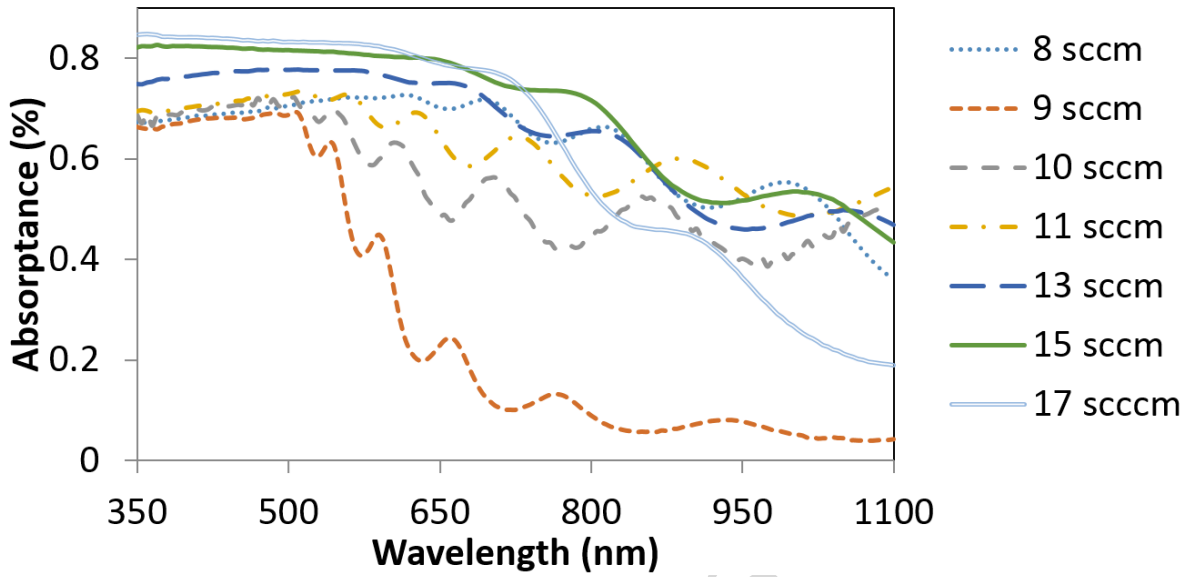

Figure 6a

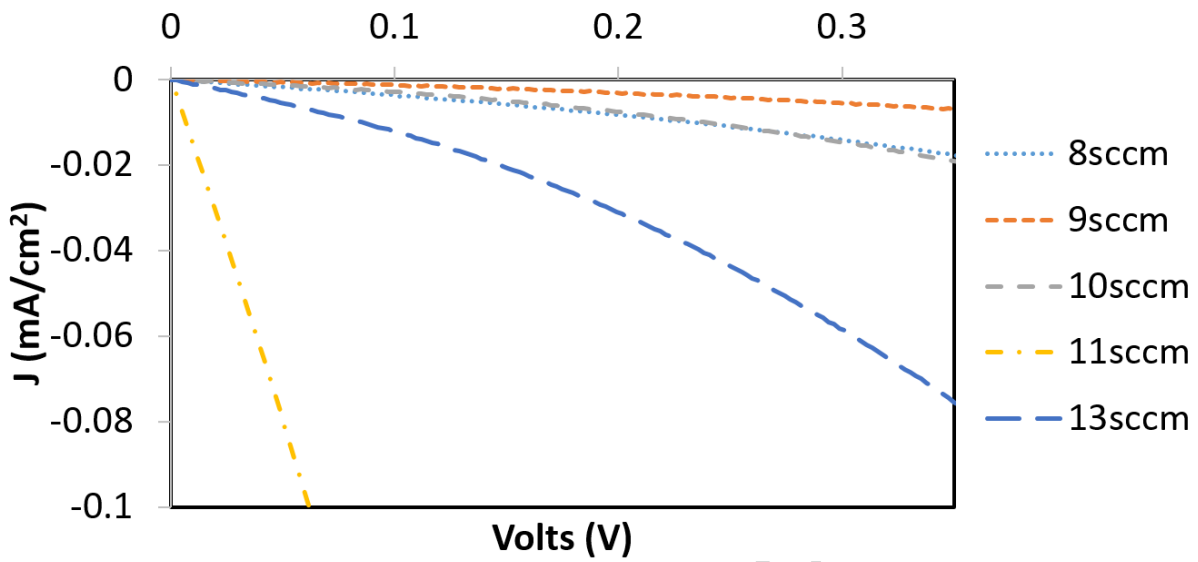

Figure 6b

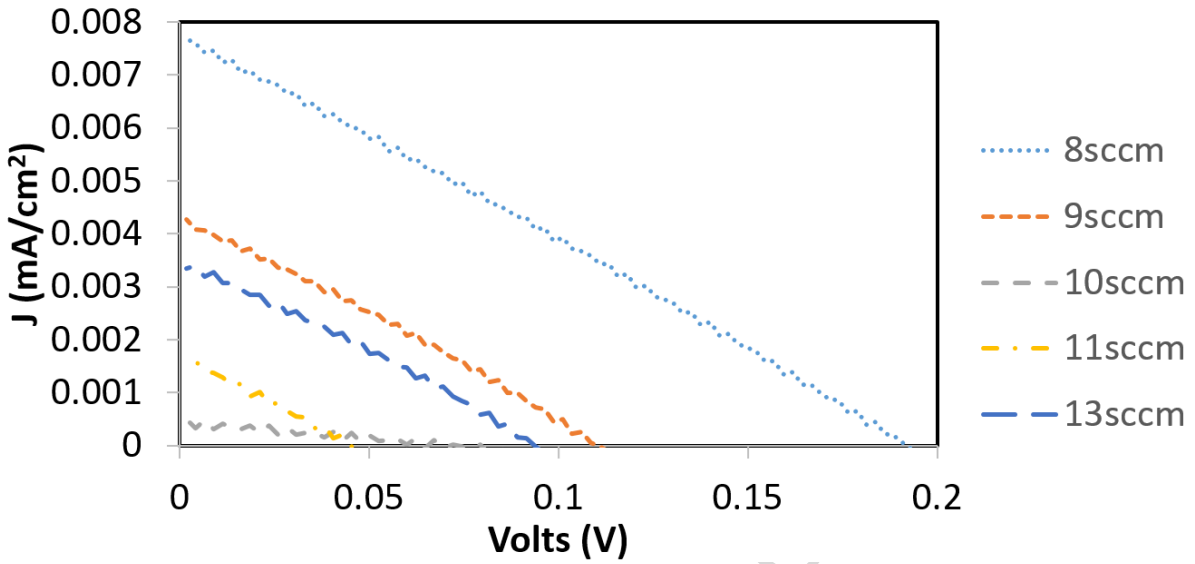

Highlights

- Under different O_2 flow rates, copper oxide films were sputtered and characterised
- Oxidation controlled by spatial separation of deposition and plasma reaction zones
- Higher O_2 flow rates during sputtering produced a less efficient solar cell
- Solar cell performance related positively to presence of crystalline Cu_4O_3 and Cu_2O